Progress In Electromagnetics Research C, Vol. 91, 253–264, 2019

Compact Complementary Folded Triangle Split Ring Resonator Triband Mobile Handset Planar Antenna for Voice and Wi-Fi Applications

P. Rajalakshmi* and N. Gunavathi

Abstract—In this work, a Complementary Folded Triangle Split Ring Resonator (CFTSRR) loaded triband mobile handset planar antenna is presented. The proposed antenna consists of a dumbbell-shaped radiating element and two CFTSRR metamaterial unit cells. The dumbbell-shaped radiating element resonates at 5 GHz. The presence of CFTSRRs additionally offers two lower band resonance. The CFTSRR-1 and CFTSRR-2 exhibit negative permittivity at 1.8 GHz and 2.4 GHz, respectively. The proposed antenna is designed to resonate at 1.8 GHz (GSM1800 MHz), 2.4 GHz, and 5 GHz (IEEE802.11ax) for voice and Wi-Fi applications of the mobile handset, respectively. The proposed antenna demonstrates compactness up to 88.6% at 1.8 GHz. The parametric studies are investigated to optimize the antenna in desired frequency bands by using Ansys HFSS19 software. The simulated and measured results are discussed. The measured result shows −10 dB reflection coefficient with bandwidth about 250 MHz (1.6 GHz–1.85 GHz), 50 MHz (2.375 GHz–2.425 GHz), and 225 MHz (4.925 GHz–5.15 GHz) which are 14.5%, 2%, and 5% respectively around their center frequencies. The measured maximum gain is approximately 1.7 dBi, 8 dBi, and 11.5 dBi for 1.8 GHz, 2.4 GHz, and 5 GHz, respectively.

1. INTRODUCTION

With the rapid growth of mobile communications technologies, portable mobile handsets are inbuilt with various wide applications such as Bluetooth, Wi-Fi, and GSM. In the future, all multiband protocols of the consumer electronic devices are integrated into a single device. There is a necessity to design a compact and multifunctional antenna for mobile handsets.

Metamaterials are artificial materials. The negative permeability and negative permittivity of the metamaterial properties help to improve the antenna performance such as size reduction, bandwidth, gain enhancement, and multiband antenna design [1–9]. In [10], the metamaterial and fractal concepts are used to design a microstrip loop antenna with poor impedance matching of −6 dB at 2.7 GHz. The electrically small planar antenna is proposed to cover either WLAN or Wi-Fi applications with low gain [11, 12]. In [13], a complicated cross-shaped patch antenna with hexagonal CSRR array is proposed only to cover Wi-Fi applications. A CPW-fed planar antenna is designed to cover only single band Wi-Fi applications [14, 15].

In the already proposed works, antennas are either large in volume, complicated in structure, or low in gain. Also, they do not cover both the Wi-Fi and GSM applications. In order to fulfill the gap, CFTSRR loaded triband patch antenna is designed, investigated, and validated in this paper for voice and Wi-Fi frequency bands of mobile handset applications with high gain and compact size.

Received 18 February 2019, Accepted 2 April 2019, Scheduled 11 April 2019

* Corresponding author: Pitchai Rajalakshmi (rajalakshmipitchai10@gmail.com).

The authors are with the Department of Electronics and Communication Engineering, National Institute of Technology, Trichy, Tamilnadu 620013, India.

This paper is organized as follows. In Sections 2 and 3, the geometry of the proposed antenna and design methodology of the CFTSRR metamaterial unit cell are presented. The parametric study of the antenna is discussed in Section 4. The simulated and measured results of the proposed antenna are given in Section 5.

2. ANTENNA DESIGN

Figure 1 shows the geometry of the proposed triband planar antenna. A low cost Flame Retardant-4 (thickness $h = 1.6\,\text{mm}$, $\varepsilon_r = 4.4$, and $\tan\delta = 0.02$) is chosen as the substrate material. Flame Retardant-4 is chosen as the substrate material. The total volume of the proposed antenna is $W \times L \times h = 16.0 \times 21.0 \times 1.6\,\text{mm}^3$.

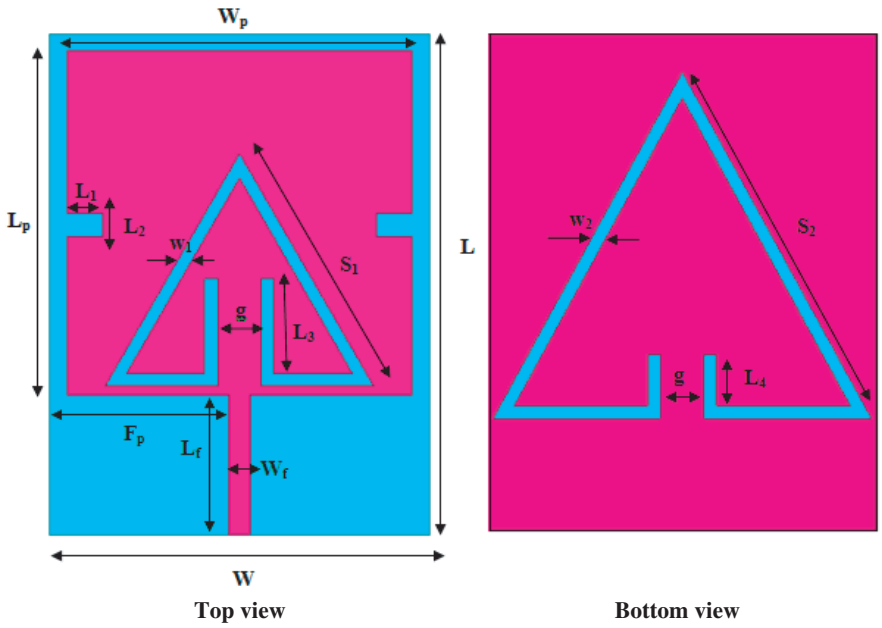

Figure 1. Geometry of the proposed antenna.

The proposed antenna is designed by the following steps. Initially, the square patch antenna is designed for 5 GHz with 50 Ω microstrip feed. However, it resonates at 5.2 GHz. In order to bring down the resonant frequency (5 GHz), the electrical length of the antenna is increased with two rectangular slots. Next CFTSRR-1 is designed for 2.4 GHz and is etched on the main radiating element to increase the electrical length for miniaturization and dual bands. Both of them cover the IEEE802.11ax applications (Wi-Fi band). Then CFTSRR-2 is etched on the ground plane of the antenna to cover GSM1800 MHz for voice applications. Finally, the proposed antenna has operating frequencies of 1.8 GHz, 2.4 GHz, and 5 GHz. Figure 2 shows the simulated reflection coefficient characteristics of the proposed antenna stage by stage.

The dimensions of the proposed antenna are considered by using transmission line theory and summarized in Table 1 [16]. At the resonant frequency (5 GHz) of the square patch antenna, the length (L_p) and width (W_p) of the patch can be calculated by:

$$L_p = W_p = \frac{c}{2f_r\sqrt{\varepsilon_{eff}}} \tag{1}$$

where c is the velocity of light, f_r the resonant frequency, and the effective permittivity ε_{eff} is given by:

$$\varepsilon_{eff} = \frac{\varepsilon_r + 1}{2} + \frac{\varepsilon_r - 1}{2}\left[1 + \frac{12h}{W_p}\right]^{\frac{-1}{2}} \tag{2}$$

where h is the thickness of the substrate, and ε_r is dielectric constant of the substrate.

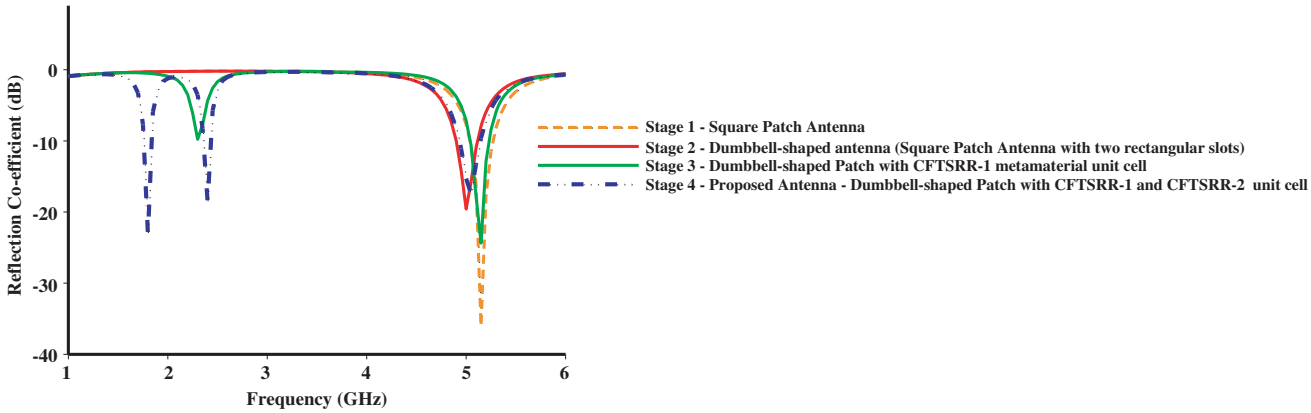

Figure 2. Simulated reflection co-efficient characteristics of the proposed antenna stage by stage.

Table 1. Summary of the dimensions of the proposed antenna.

Parameter	Value (mm)	Parameter	Value (mm)
L	21	S_2	9
W	16	L_1	1.5
L_p & W_p	14.5	L_2	1
F_p	7.55	L_3	4
L_f	5.86	L_4	2.5
W_f	2.8	w_1 & w_2	1
S_1	6.5	g	1.5

3. CFTSRR METAMATERIAL UNIT CELL DESIGN METHODOLOGY

Two different CFTSRR metamaterial unit cells are designed for 1.8 GHz and 2.4 GHz, respectively. CFTSRR-1 is etched on the top of the patch which is used to attain a lower band of the IEEE802.11ax. CFTSRR-2 metamaterial unit cell is etched on the ground plane of the substrate which is resonated at GSM1800 frequency band. These metamaterial unit cells act as a radiating element in the patch, which are used for miniaturization.

The resonant frequency (f) of CFTSRR metamaterial unit cells is calculated by the following equations [17].

$$L_{eq} = \frac{3\mu_0\mu_r}{2\pi}\left(\ln\left(\frac{S}{w}\right) - 1.405\right) \tag{3}$$

$$C_{eq} = 0.75SC_{pul} \tag{4}$$

$$f = \frac{1}{2\pi\sqrt{L_{eq}C_{eq}}} \tag{5}$$

$$C_{pul} = \frac{\sqrt{\varepsilon_{eff}}}{cZ_0} \tag{6}$$

L_{eq} and C_{eq} are the total inductance and capacitance of the metamaterial unit cells, respectively. S is the side of the outer triangle of the unit cell. C_{pul} and Z_0 are the per unit length capacitance between the rings and impedance of the medium, respectively. w is the width of the ring. c is the velocity of light.

The unit cell is constructed with a complementary folded triangle split ring resonator as shown in the bottom view of Figure 1. The metamaterial performance is investigated by transverse electromagnetic

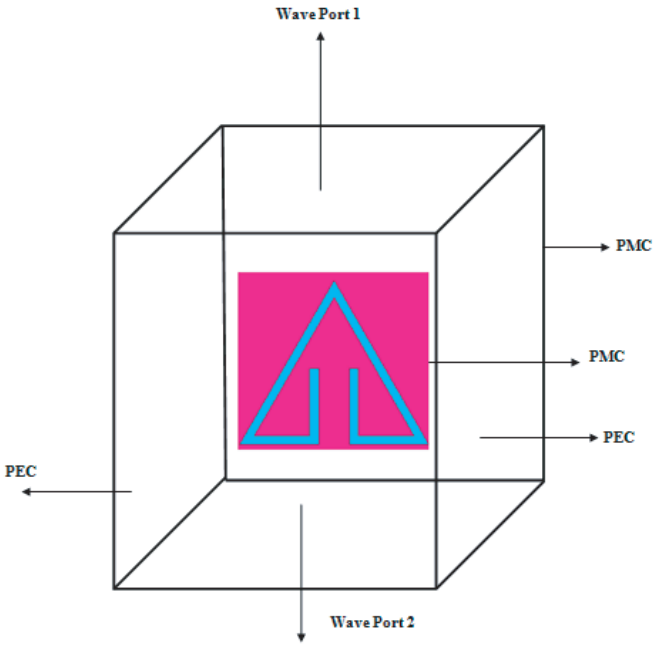

Figure 3. Simulation waveguide setup of the CFTSRR metamaterial unit cell.

(TEM) mode. Perfect Electric Conductor (PEC) and Perfect Magnetic Conductor (PMC) boundary are assigned in x and y-directions, respectively. The electromagnetic wave is propagated in z-direction. The simulation setup of the CFTSRR metamaterial unit cell is shown in Figure 3.

The effective parameters of the proposed unit cell are extracted by using the transmission-reflection method [18]. The reflection coefficient (Γ) is calculated as

$$\Gamma = \frac{z_0 - 1}{z_0 + 1} \tag{7}$$

where z_0 is the relative impedance determined as the square root of the ratio of effective permeability and permittivity.

$$z_0 = \sqrt{\frac{\mu_r}{\varepsilon_r}} \tag{8}$$

The reflection coefficient (S_{11}) and transmission coefficient (S_{21}) can be determined as

$$S_{11} = \frac{\left(1 - \Gamma^2\right) z}{1 - \Gamma^2 z^2} \tag{9}$$

$$S_{21} = \frac{\left(1 - z^2\right) \Gamma}{1 - \Gamma^2 z^2} \tag{10}$$

$z = e^{-}jk_0d$ is the propagation vector. The effective parameters such as relative permittivity (ε_r) and permeability (μ_r) can be retrieved using S_{11} and S_{21} by using Nicolson-Ross-Weir approach. The equation is as follows

$$\mu_r = \frac{2}{jk_0d} * \frac{1 - V_2}{1 + V_2} \tag{11}$$

$$\varepsilon_r = \frac{2}{jk_0d} * \frac{1 - V_1}{1 + V_1} \tag{12}$$

$$V_1 = S_{21} + S_{11} \tag{13}$$

$$V_2 = S_{21} - S_{11} \tag{14}$$

$$S_{11} = \mathrm{re}(S_{11}) + j(\mathrm{im}(S_{11})) \tag{15}$$

$$S_{21} = \text{re}(S_{21}) + j(\text{im}(S_{21})) \tag{16}$$

where $k_0 = 2\pi/\lambda$ is a wave number, and d is the slab thickness.

S_{11} and S_{21}-parameters of the CFTRR metamaterial unit cell are obtained from the HFSS and shown in Figures 4(a) and 4(b). The negative permittivity (ε) characteristics are retrieved from S_{11} and S_{21} of the CFTSRR-1 and CFTSRR-2 metamaterial unit cell structures using MATLAB code. The negative permittivities of the proposed CFTSRR-1 and CFTSRR-2 at 2.4 GHz & 1.8 GHz are shown in Figures 5(a) and 5(b), respectively.

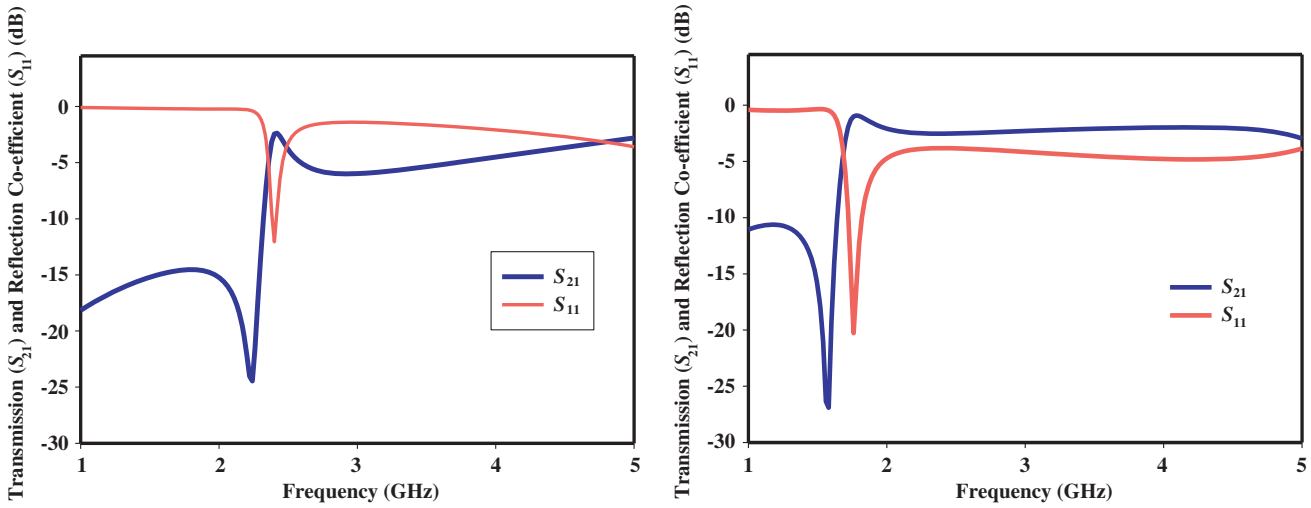

Figure 4. Unit cell simulation response of the CFTSRR metamaterial unit cells. (a) CFTSRR-1 at 2.4 GHz, (b) CFTSRR-2 at 1.8 GHz.

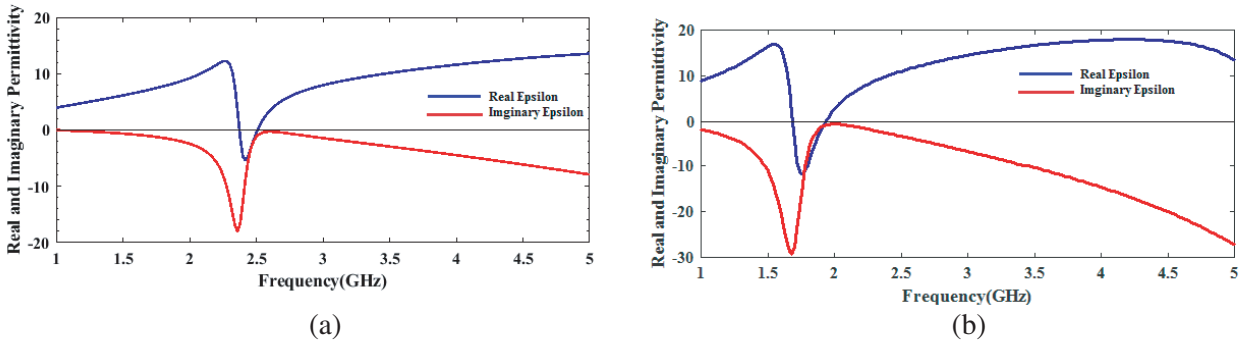

Figure 5. Negative permittivity of the CFTSRR metamaterial unit cells. (a) CFTSRR-1 at 2.4 GHz, (b) CFTSRR-2 at 1.8 GHz.

4. PARAMETRIC STUDY OF THE PROPOSED ANTENNA

4.1. Effect of Patch Length (L_p) Variations

Figure 6 illustrates the frequency behavior of the antenna reflection coefficient characteristics when the length of the patch (L_p) varies from 11.5 mm to 14.5 mm, with the other parameters being constant. As the length of the patch (L_p) decreases, the resonant frequency of the third band moves forward. The patch length (L_p) mainly controls the higher frequency band of IEEE802.11 ax. The length of the patch (L_p) at 14.5 mm gives the resonant frequency at 5 GHz with good impedance matching of −18 dB.

4.2. Effect of Width (w_1) on CFTSRR-1

Figure 7 shows the frequency behavior of the reflection coefficient characteristics when the width ($\mathbf{w_1}$) of CFTSRR-1 varies from 0.6 mm to 1.4 mm, with the other parameters kept constant. Figure 7 shows that the second resonant frequency moves forward as the width of CFTSRR-1 ($\mathbf{w_1}$) is increased. Therefore, the width ($\mathbf{w_1}$) of CFTSRR-1 is set to 1.0 mm so as to assure resonant frequency at 2.4 GHz with good impedance matching of −19 dB.

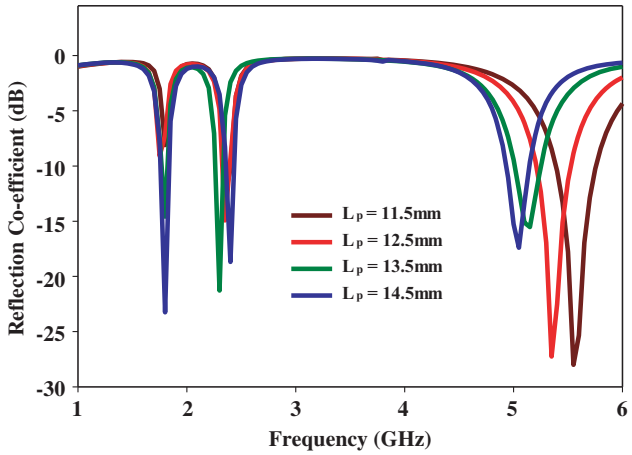

Figure 6. Simulated reflection co-efficient characteristics of various L_p.

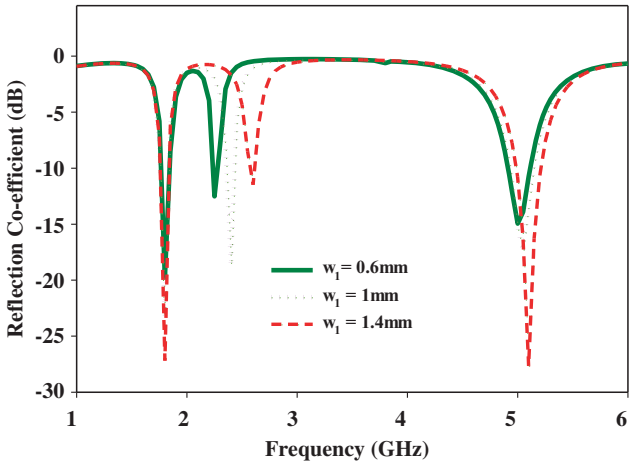

Figure 7. Simulated reflection co-efficient characteristics of various w_1.

4.3. Effect of Width (w_2) on CFTSRR-2

Figure 8 shows simulated reflection coefficient characteristics of the proposed antenna when the width ($\mathbf{w_2}$) of CFTSRR-2 varies from 0.5 mm to 2 mm, with the other parameters kept constant. Figure 8 illustrates that the first resonant frequency moves downward as the width of the CFTSRR-2(w2) is decreased. Specifically, when the width of CFTSRR-2 ($\mathbf{w_2}$) is maintained as 1 mm, the first resonance of the proposed antenna is obtained at 1.8 GHz with good impedance matching, thus parameter $\mathbf{w_2}$ value is finally set as 1 mm.

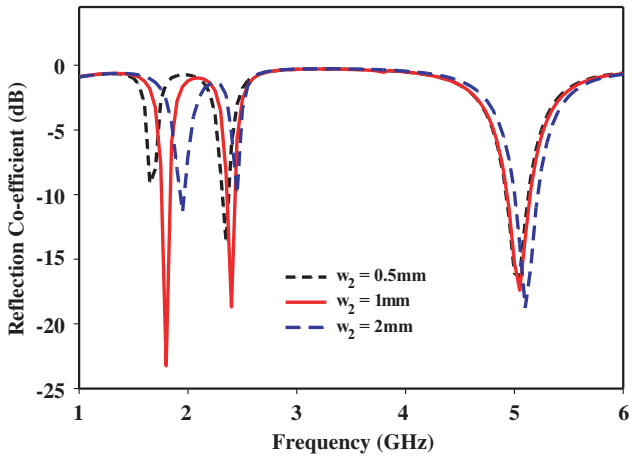

Figure 8. Simulated reflection co-efficient characteristics of various w_2.

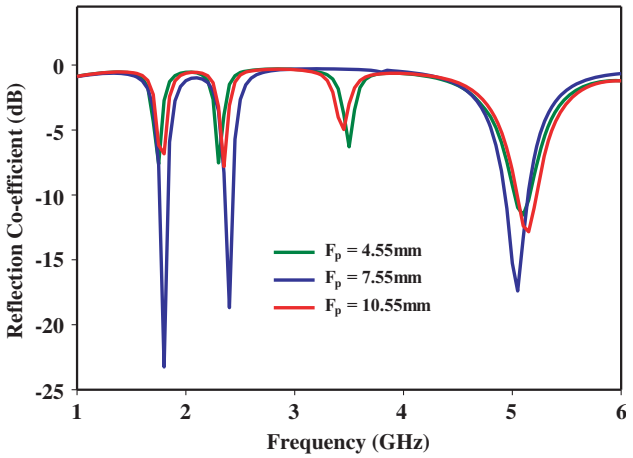

Figure 9. Simulated reflection co-efficient characteristics of various feed position (F_p).

4.4. Effect of Feed Position (F_p) of the Proposed Antenna

Figure 9 shows the simulated reflection coefficient characteristics of various feed positions (F_p) of the proposed antenna. When the feed position (F_p) shifts from 4.55 mm to 10.55 mm with the step size of 1 mm, the proposed antenna provides a good impedance matching at 7.55 mm. Therefore, the feed position of (F_p) is set to 7.55 mm so as to assure the triple resonant frequencies such as 1.8 GHz, 2.4 GHz, and 5 GHz with good impedance matching of −24 dB, −19 dB, and −18 dB respectively.

5. RESULTS AND DISCUSSION

The fabricated prototype of the proposed antenna is shown in Figure 10. The proposed antenna is measured using Agilent PNA 8362B vector network analyzer. The simulated and measured reflection coefficient characteristics of the proposed antenna are shown in Figure 11. Due to soldering and fabrication effects, there is a little discrepancy between the simulated and measured results.

The simulated and measured radiation patterns on the x-z plane (E-plane) and x-y plane (H-plane) for 1.8 GHz, 2.4 GHz, and 5 GHz are shown in Figures 12(a), (b), and (c), respectively. Both simulation and measurement results show that the proposed antenna exhibits omnidirectional radiation pattern in the H-plane (x-y plane) at the respective bands of the proposed antenna. The E-plane radiation pattern (x-z plane) is directional at 1.8 GHz and 2.4 GHz, and broadside directional at 5 GHz.

Figures 13(a), (b), and (c) show the simulated gain of the resonating respective bands of the

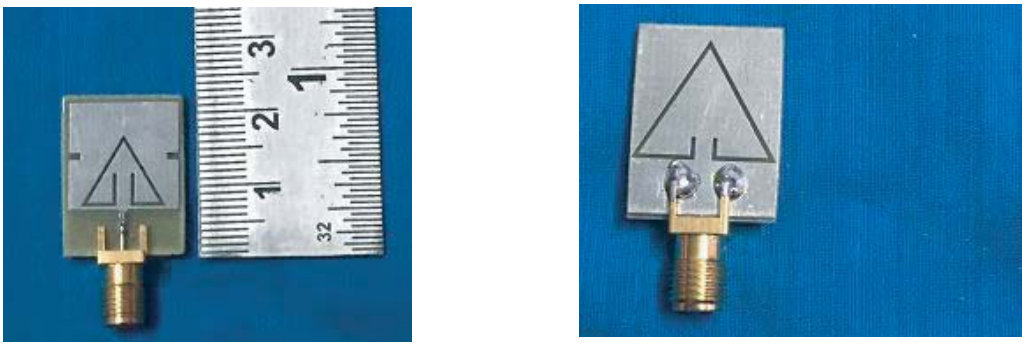

Figure 10. Photograph of the proposed antenna.

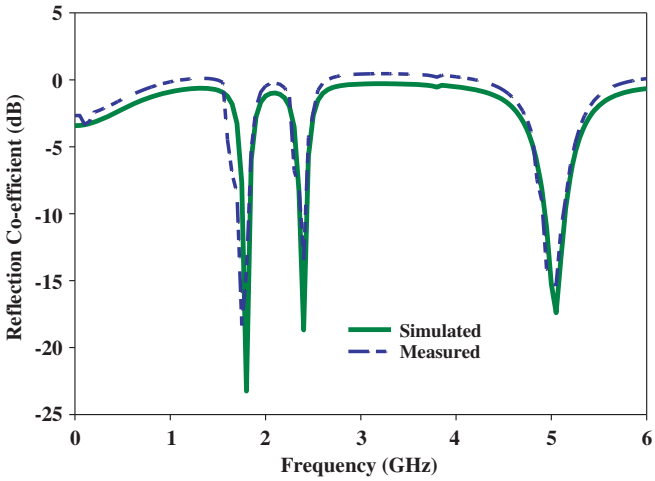

Figure 11. Simulated and measured reflection co-efficient characteristics of the proposed antenna.

proposed antenna such as 1.8 GHz, 2.4 GHz, and 5 GHz, respectively. The simulated gains of the various evolution stages of the proposed antenna are tabulated in Table 2. To obtain the antenna's resonant mode characteristics, the simulated current distribution should be obtained at 1.8 GHz, 2.4 GHz, and 5 GHz as shown in Figure 14. The surface current distribution is observed in front and back of the CFTSRR metamaterial unit cells at 1.8 GHz and 2.4 GHz, respectively. At 5 GHz, the current distribution is good between dumbbell-shaped radiating element and microstrip feed.

The proposed antenna is compared with existing antennas and summarized in Table 3, which shows that the proposed antenna is miniaturized with three operating bands and provides the highest gain at 5 GHz [4, 8, 10, 11, 13].

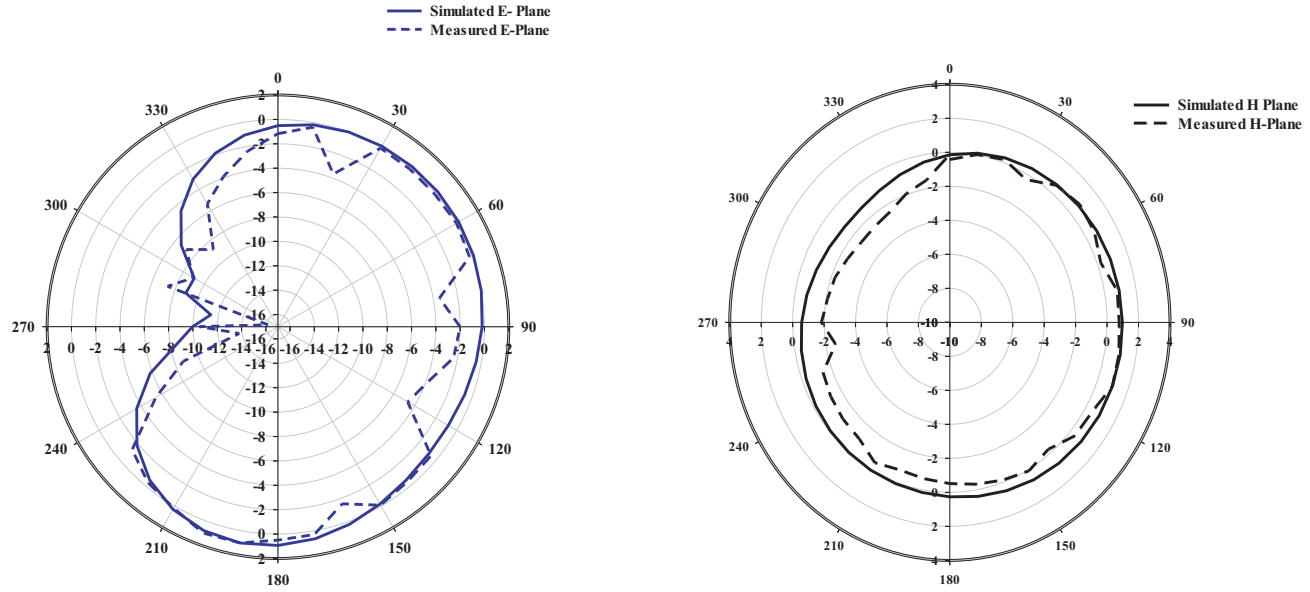

(a)

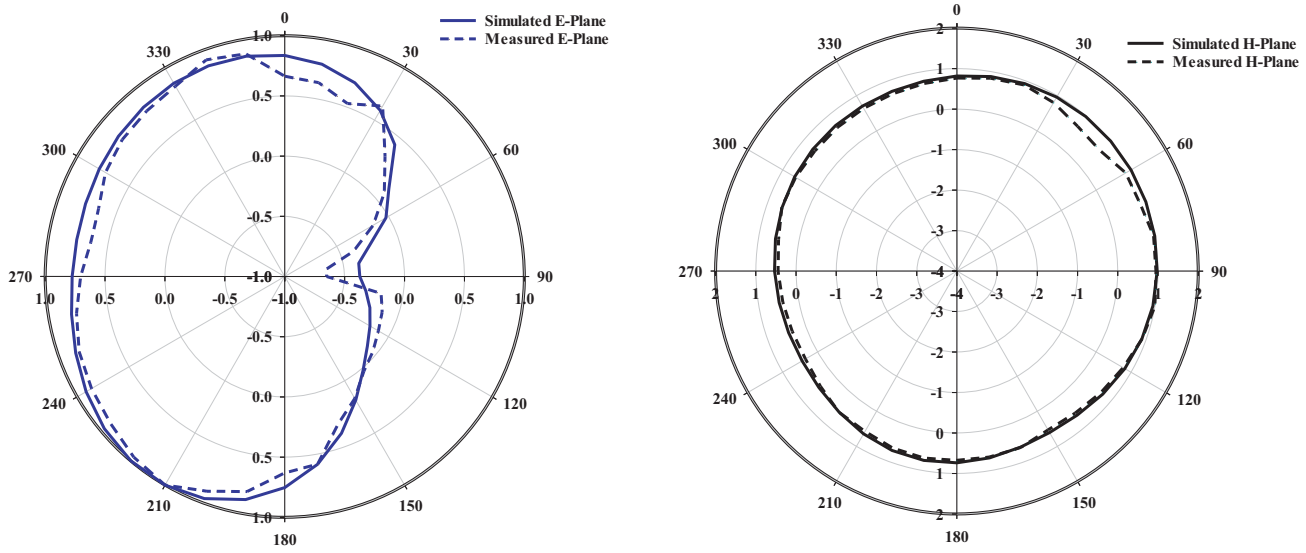

(b)

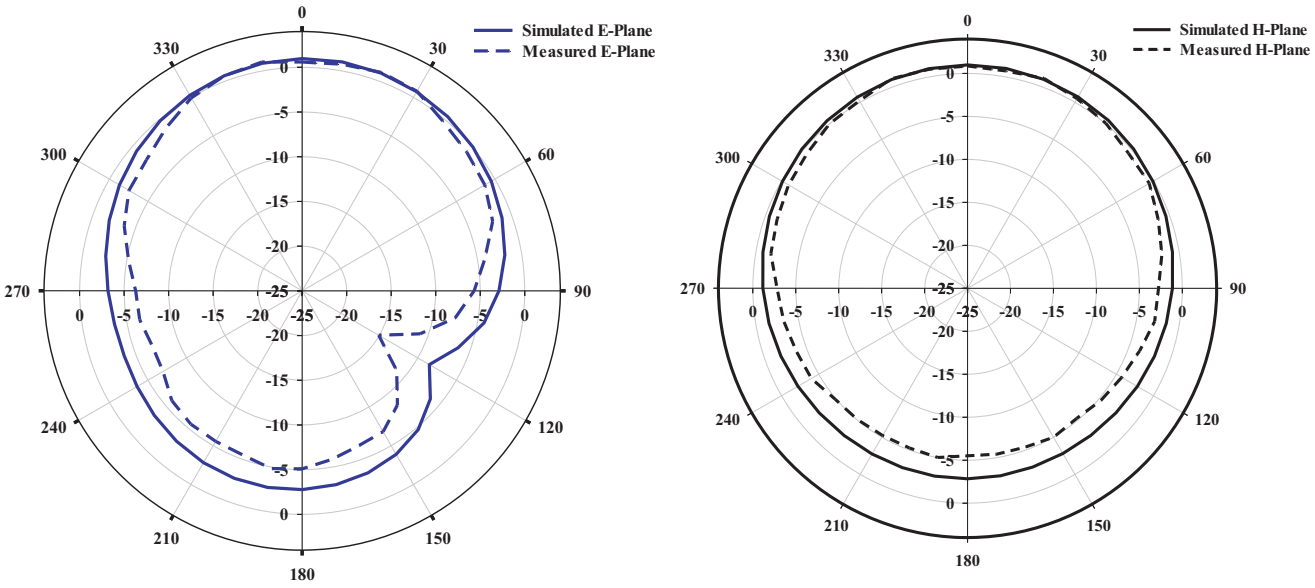

(c)

Figure 12. (a) Radiation pattern at 1.8 GHz. (b) Radiation pattern at 2.4 GHz. (c) Radiation pattern at 5 GHz.

Table 2. Comparison of various evolution stages of proposed antenna for Voice and Wi-Fi applications.

S. No	Evolution stages	Resonant Frequency (GHz)	Simulated Gain (dBi)
1	Dumb bell Shaped Antenna	5	2.93 dB
2	CFTSRR-1 Loaded Patch Antenna	2.35 & 5	4.34/11.7 dB
3	CFTSRR-1 & CFTSRR-2 Loaded Patch Antenna	1.8, 2.4 & 5	2.76/10.04/13.3 dB

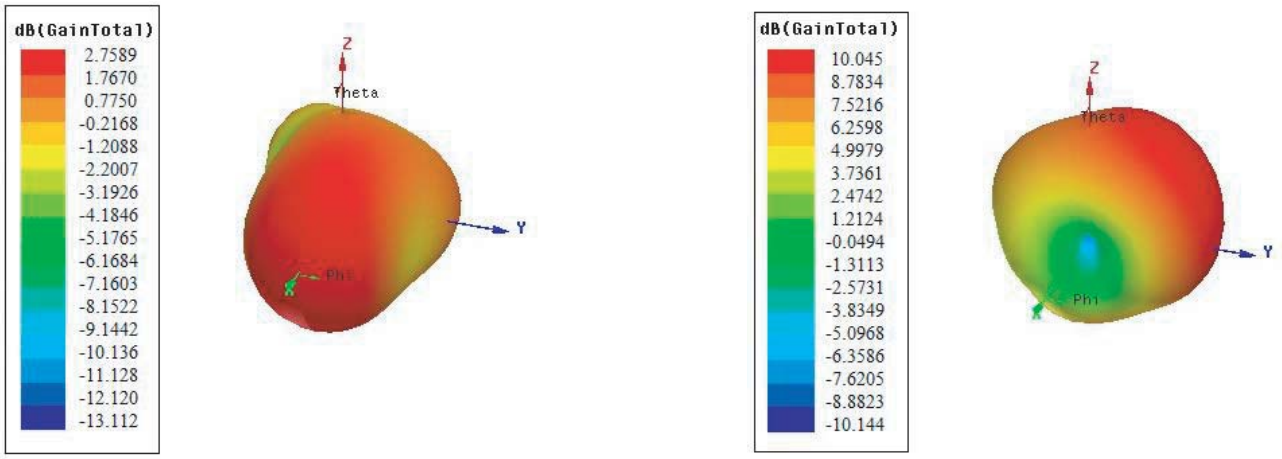

(a) (b)

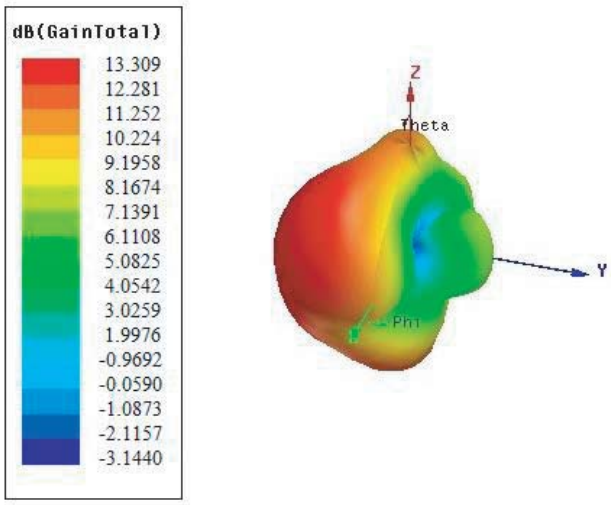

(c)

Figure 13. (a) Simulated gain at 1.8 GHz. (b) Simulated gain at 2.4 GHz. (c) Simulated gain at 5 GHz.

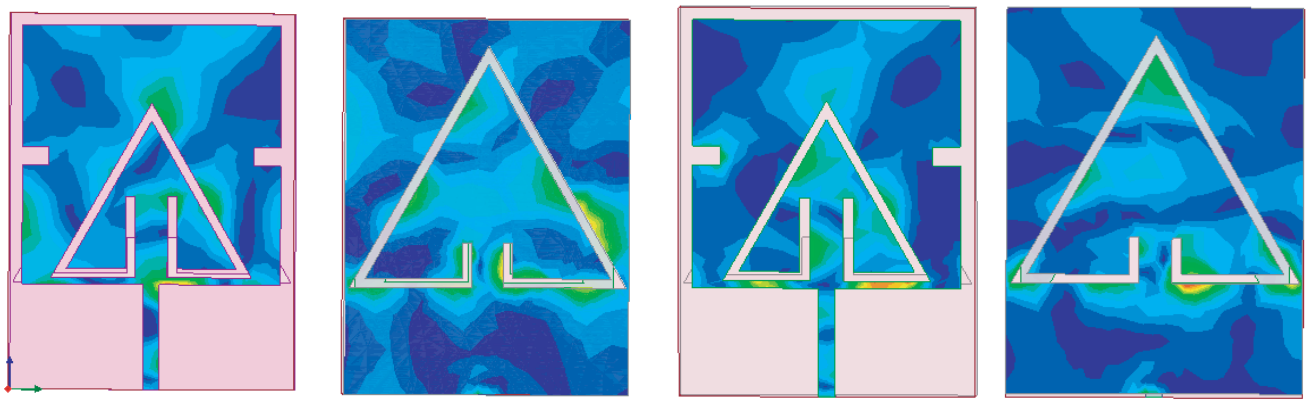

(a) (b)

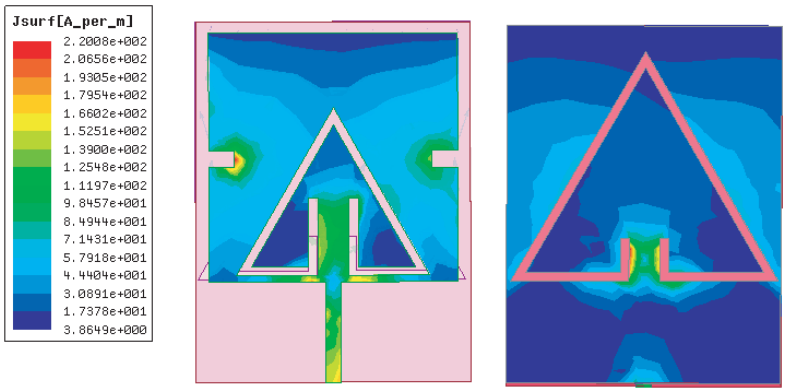

(c)

Figure 14. Simulated current distribution at (a) 1.8 GHz, (b) 2.4 GHz, (c) 5 GHz.

Table 3. Comparison between the proposed antenna with existing antennas in terms of size, resonant frequency and gain.

Reference	Year	Patch Dimensions $((W \times L \times h)\,\mathbf{mm^3})$	Frequency (GHz)	Measured Gain
[4]	2018	$60 \times 60 \times 0.8$	5.4–5.8 GHz	10 dBi
[8]	2018	$20 \times 30 \times 1.6$	2.4–2.5 GHz	1.92 dBi/1.75 dBi
[10]	2018	$40 \times 40 \times 1.6$	2.7/4.5/5.9	3.5 dBi/4.5 dBi/4.2 dBi
[11]	2018	$12.5 \times 13.05 \times 0.8$	2.4/5	1.062 dBi/1.55 dBi
[13]	2018	$20 \times 25 \times 1.6$	2.4/5	6 dBi/10 dBi
Proposed		$16 \times 21 \times 1.6$	1.8/2.4/5	1.7 dBi/8 dBi/11.5 dBi

6. CONCLUSION

A compact CFTSRR metamaterial loaded planar antenna is proposed for mobile handset applications such as voice and Wi-Fi frequency bands. The CFTSRRs introduce another two resonances in the lower Wi-Fi (IEEE802.11 ax) bands and voice (GSM1800 MHz) frequency bands, respectively. The effective permittivity of CFTSRR metamaterial cells characteristics is retrieved. It is seen that the metamaterial loading achieves gain enhancement and triple band operations such as 1.8 GHz, 2.4 GHz, and 5 GHz with compact dimensions of $16.0 \times 21.0 \times 1.6\,\mathrm{mm}^3$. The parametric study is done to validate the results. A prototype antenna is fabricated and characterized. Moreover, electrically small size and low cost make the antenna ideally applicable to present and future mobile handset devices.

REFERENCES

1. Caloz, C. and T. Itoh, *Electromagnetic Metamaterials: Transmission Line Theory and Microwave Applications*, 1st Edition, Wiley-IEEE Press, Hoboken, NJ, 2006, ISBN-10: 0471669857.
2. Marqués, R., F. Martn, and M. Sorolla, *Metamaterials with Negative Parameters: Theory, Design and Microwave Applications*, Hoboken, NJ, Wiley, 2007, ISBN: 978-0-471-74582-2.
3. Ji, J. K., G. H. Kim, and W. M. Seong, "Bandwidth enhancement of metamaterial antennas based on composite right/left handed transmission line," *IEEE Antennas and Wireless Propagation Letters*, Vol. 9, 36–39, 2010.
4. Chen, Q., H. Zhang, Y.-J. Shao, and T. Zhong, "Bandwidth and gain improvement of an L-shaped slot antenna with metamaterial loading," *IEEE Antennas and Wireless Propagation Letters*, Vol. 17, 1411–1415, 2018.
5. Roy, S. and U. Chakraborty, "Gain enhancement of a dual-band WLAN microstrip antenna loaded with diagonal pattern metamaterials," *IET Communications*, Vol. 12, No. 12, 1448–1453, 2018.
6. Joshi, J. G., S. S. Pattnaik, S. Devi, and M. R. Lohokare, "Frequency switching of electrically small patch antenna using metamaterial loading," *Indian Journal of Radio & Space Physics*, Vol. 40, 159–165, 2011.
7. Chou, Y.-J., G.-S. Lin, J.-F. Chen, L.-S. Chen, and M.-P. Houng, "Design of GSM/LTE multiband application for mobile phone antennas," *Electronics Letters*, Vol. 51, No. 17, 1304–1306, 2015.
8. Sharma, M., N. Mishra, and R. K. Chaudhary, "SRR based compact wideband metamaterial inspired antenna for WiMAX (2.5–2.7)/WLAN (2.4–2.48)/Bluetooth (2.4–2.48)/LTE (2.3–2.4) applications," *Progress In Electromagnetics Research Letters*, Vol. 80, 109–116, 2018.
9. Sameer, K., M. Sharma, A. Abdalla, and Z. Hu, "Miniaturisation of an electrically small metamaterial inspired antenna using additional conducting layer," *IET Microwaves, Antennas & Proagation*, Vol. 12, No. 8, 1444–1449, 2018.

10. Varamini, G., A. Keshtkar, and M. Naser-Moghadasi, "Miniaturization of microstrip loop antenna for wireless applications based on metamaterial metasurface," *International Journal of Electronics and Communications (AEU)*, Vol. 83, 32–39, 2018.
11. Liu, W., L. Xu, and H. Zhan, "Design of 2.4 GHz/5 GHz planar dual-band electrically small slot antenna based on impedance matching circuit," *International Journal of Electronics and Communications (AEÜ)*, Vol. 83, 322–328, 2018.
12. Zhu, X., Y. Gu, and W. Wu, "A novel dual band antenna for wireless applications," *IEEE Antennas and Wireless Propagation Letters*, Vol. 15, 516–519, 2016.
13. Rajalakshmi, P. and N. Gunavathi, "Gain enhancement of cross shaped patch antenna for IEEE 802.11ax Wi-Fi applications," *Progress In Electromagnetics Research Letters*, Vol. 80, 91–99, 2018.
14. Gunavathi, N. and D. Sriram Kumar, "Miniaturized unilateral coplanar waveguide-fed asymmetric planar antenna with reduced radiation hazards for 80.11ac application," *Microwave and Optical Technology Letters*, Vol. 58, No. 2, 337–342, 2015.
15. Gunavathi, N. and D. Sriram Kumar, "CPW-fed monopole antenna with reduced radiation hazards towards human head using metallic thin-wire mesh for 802.11ac application," *Microwave and Optical Technology Letters*, Vol. 57, No. 11, 2684–2687, 2015.
16. Balanis, C. A., *Antenna Theory Analysis and Design*, 2nd Edition, John Wiley & Sons, New York, 1997.
17. Vidyalakshmi, M. R., B. Rekha, and P. H. Rao, "Stopband characteristics of complementary triangular split ring resonator loaded microstrip line," *2011 IEEE Applied Electromagnetics Conference (AEMC)*, 2011.
18. Smith, D. R., S. Schultz, P. Markos, and C. M. Soukoulis, "Determination of negative permittivity and permeability of metamaterials from reflection and transmission coefficients," *Phys. Rev. B*, Vol. 65, 195104, 2002.